Well-Distributed Pt-Nanoparticles within Confined Coordination Interspaces of Self-Sensitized Porphyrin Metal-Organic Frameworks: Synergistic Effect Boosting Highly Efficient Photocatalytic Hydrogen Evolution Reaction

Shuai Li, Hong-Min Mei, Shi-Lin Yao, Zhi-Yao Chen, Yu-Lin Lu, Li Zhang*, Cheng-Yong Su*

MOE Laboratory of Bioinorganic and Synthetic Chemistry, Lehn Institute of Functional Materials, School of Chemistry, Sun Yat-Sen University, Guangzhou 510275, China

E-mail: zhli99@mail.sysu.edu.cn; cesscy@mail.sysu.edu.cn

Contents

Captions for Figures and Tables

1. Comparison of H_2 Evolution Rates of Different MOF Composites

Table S1. Comparison of H_2 evolution rates of different MOF composites under visible light irradiation.

Catalyst	Co-catalyst	Photosensitizer	Light source (nm)	H_2 production rate ($\mu mol \cdot g^{-1} \cdot h^{-1}$)	TON and TOF (based on Pt NPs)	Reference
MIL-100(Fe)	Pt NPs	None	≥ 420	98	TON = 23.97 TOF = 2.66 h^{-1}	*New J. Chem.* **2016**, *40*, 9170-9175
UiO-66-NH_2(Zr)	Pt NPs	None	> 380	257	TON = 17.48 TOF = 1.75 h^{-1}	*Angew. Chem. Int. Ed.* **2016**, *55*, 9389-9393
MIL-125-NH_2(Ti)	Pt NPs	None	> 420	367		*J. Phys. Chem. C* **2012**, *116*, 20848-20853
Al-TCPP	Pt NPs	None	> 380	129	TON = 573.2 TOF = 35.8 h^{-1}	*Adv. Mater.* **2018**, *30*, 1705112
Al-PMOF	Pt NPs	None	≥ 420	200	TON = 22 TOF = 4 h^{-1}	*Angew. Chem. Int. Ed.* **2012**, *51*, 7440-7444
USTC-8 (In)	Pt NPs	None	> 380	341	TON = 66.54 TOF = 4.5 h^{-1}	*ACS Catal.* **2018**, *8*, 4583-4590
UiO-66(Zr)	Pt NPs	Rhodamine B	≥ 420	116	TON = 33.99 TOF = 2.26 h^{-1}	*Chem. Commun.* **2014**, *50*, 7063-7066
MIL-101-NH_2(Cr)	Pt NPs	Rhodamine B	≥ 420	477	TON = 247 TOF = 8.23 h^{-1}	*Chem. Commun.* **2014**, *50*, 11645-11648
Pt@MIL-125/Au	Pt NPs	None	> 380	1743	TON = 416.31 TOF = 69.38 h^{-1}	*Angew. Chem. Int. Ed.* **2018**, *57*, 1103-1107
MIL-101/CdS	Pt NPs	None	> 420	7550	TON = 4582.7 TOF = 294.5 h^{-1}	*Chem. Commun.* **2013**, *49*, 6761-6763
Pt@Pd-PCN-222(Hf)	Pt NPs	None	≥ 420	22674	TON = 4131.2 TOF = 482.5 h^{-1}	This work

2. General Information

All reagents and solvents used in this work were purchased from commercial supplies without further purification. Powder X-ray diffraction (PXRD) studies were carried out on a Rigaku Smart Lab diffractometer (Bragg-Brentano geometry, Cu-Kα1 radiation, λ = 1.54056 Å). UV–vis spectra were tested on a Shimadzu/UV-3600 spectrophotometer. Inductively coupled plasma optical emission spectrometer (ICP-OES) were measured on Thermo ICAP Qc. Gas and vaper adsorption measurements were carried out using a Quantachrome Autosorb-iQ2 and Autosorb-iQ-MP-VP analyzer, respectively. Prior to an adsorption measurement, samples were typically heated at 150℃ under vacuum for 18 h to remove the adsorbed solvent molecules. Scanning electron microscopy (SEM) analysis was performed using a Quanta 400F. Samples for SEM tests were dispersed in EtOH with the aid of sonication, and then deposited on a conductive tape. Transmission electron microscopy (TEM) investigations, energy dispersive X-ray (EDX) elemental mapping and high-angle annular dark-field scanning TEM (HAADF-STEM) were performed by JEM-ARM200P. Prior to TEM measurements, samples were dispersed in EtOH using a sonication method, and then mounted on a carbon coated copper grid. Tomographic experiments were performed on Leica EM UC6/FC6, and the epoxy resin act as embedding medium. X-ray photoelectron spectroscopy (XPS) measurement was performed on a ULVAC PHI Quantera microprobe. Electrochemical measurement was performed on a CHI 660e electrochemical workstation.

3. Physical Characterizations

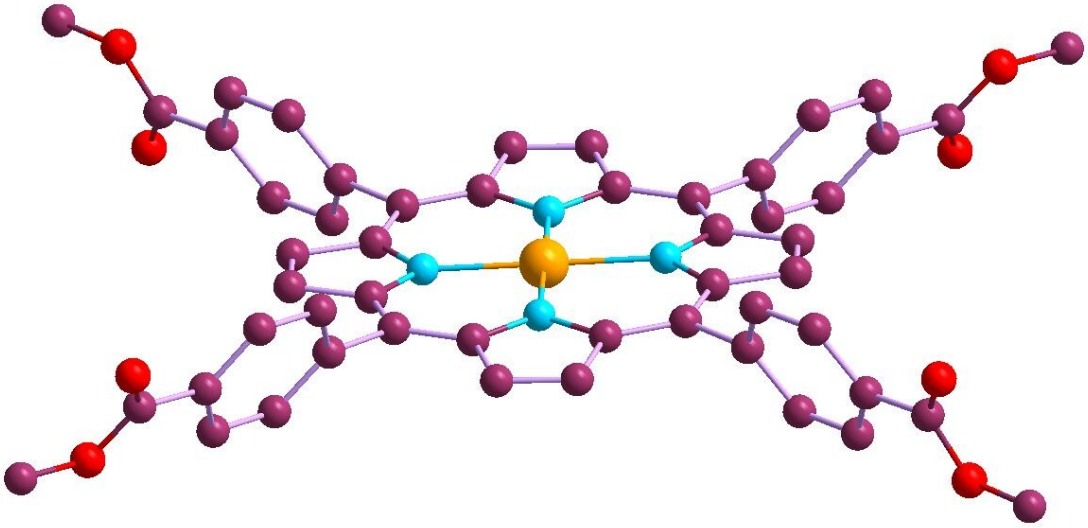

Figure S1. The crystal structure of PdTMCPP.

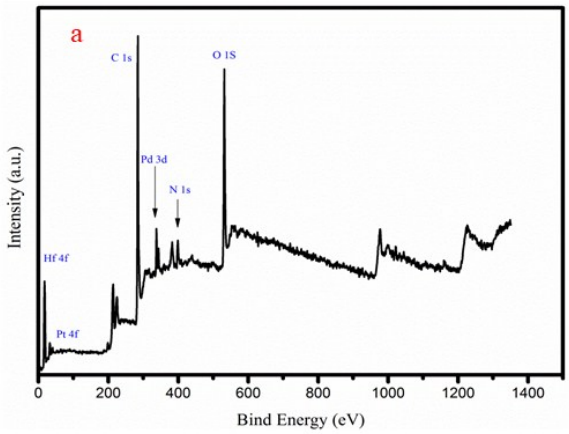

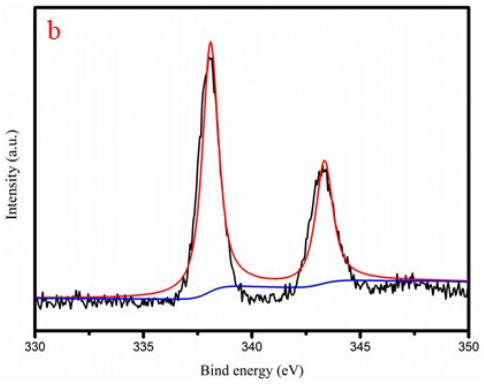

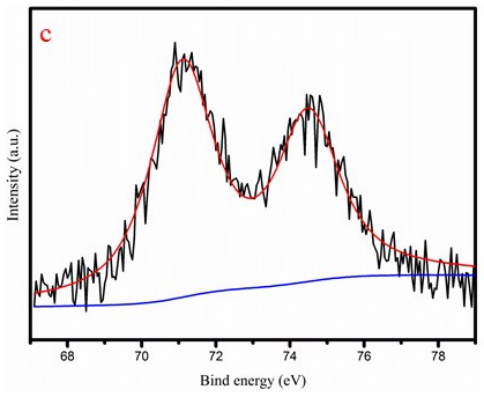

Figure S2. XPS spectrum of Pt@Pd-PCN-222(Hf).

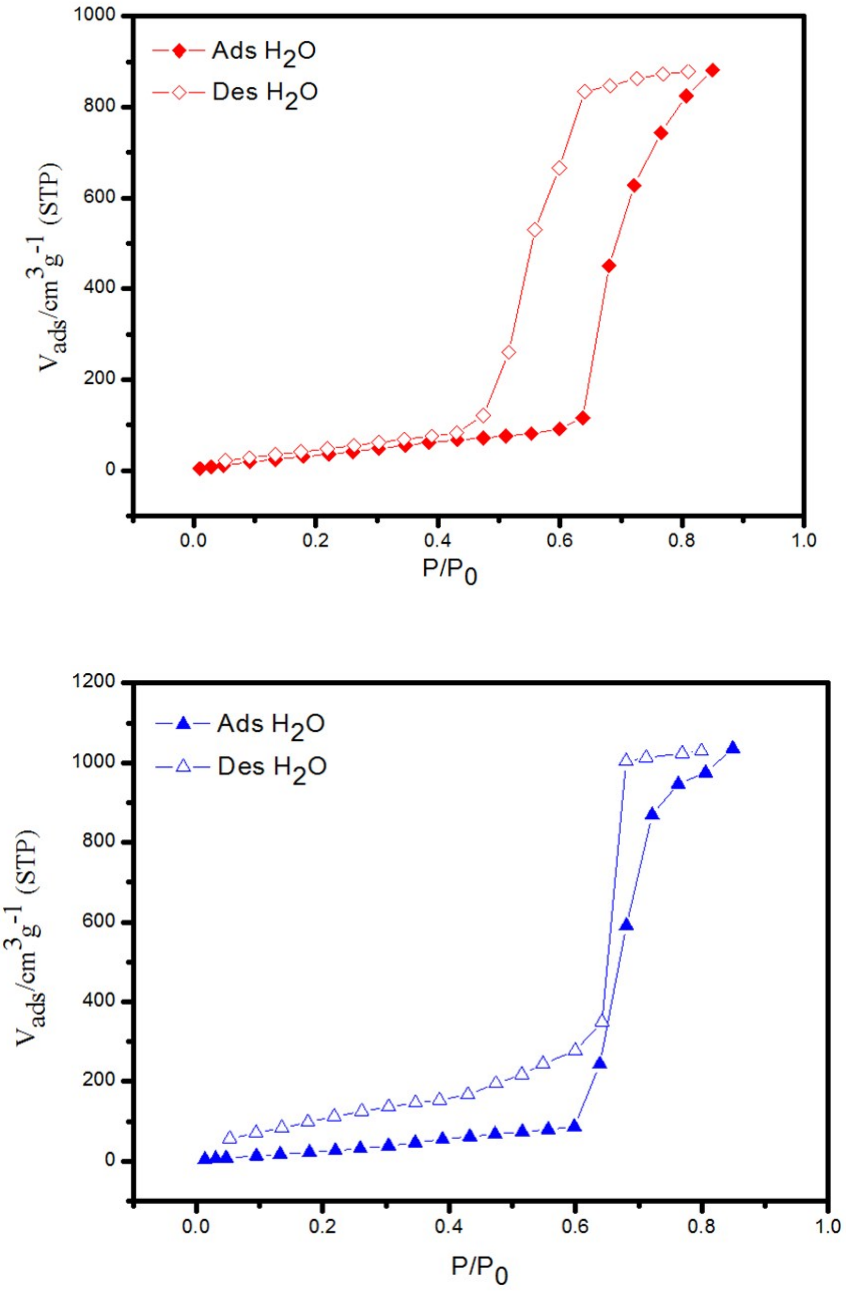

Figure S3. Water sorption isotherms of Pd-PCN-222(Hf) (up) and Pt@Pd-PCN-222(Hf) (down).

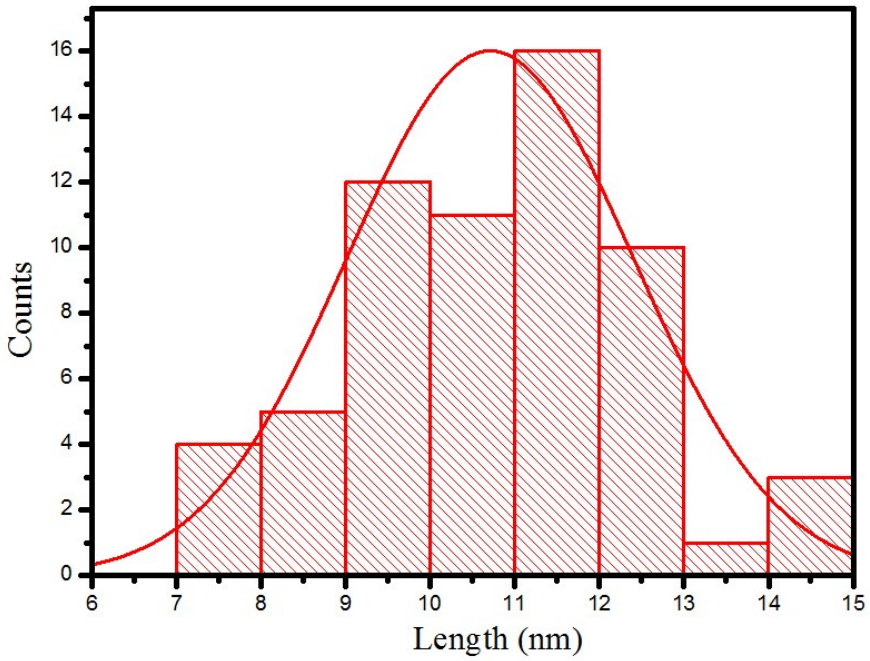

Figure S4. Particle size distribution of Pt NPs along the length.

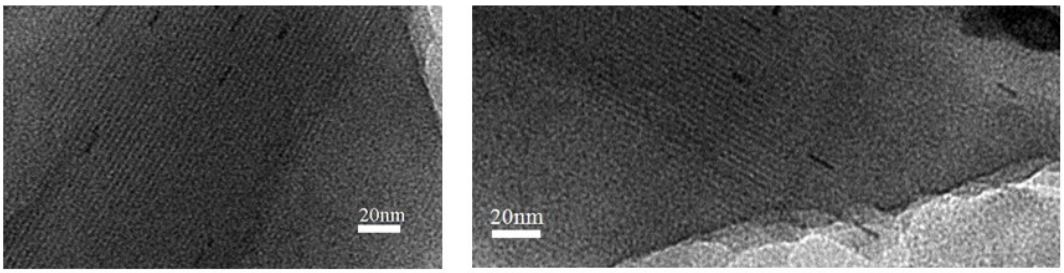

Figure S5. The electron tomographic reconstruction of Pt@Pd-PCN-222(Hf).

4. Chemical Stability Study

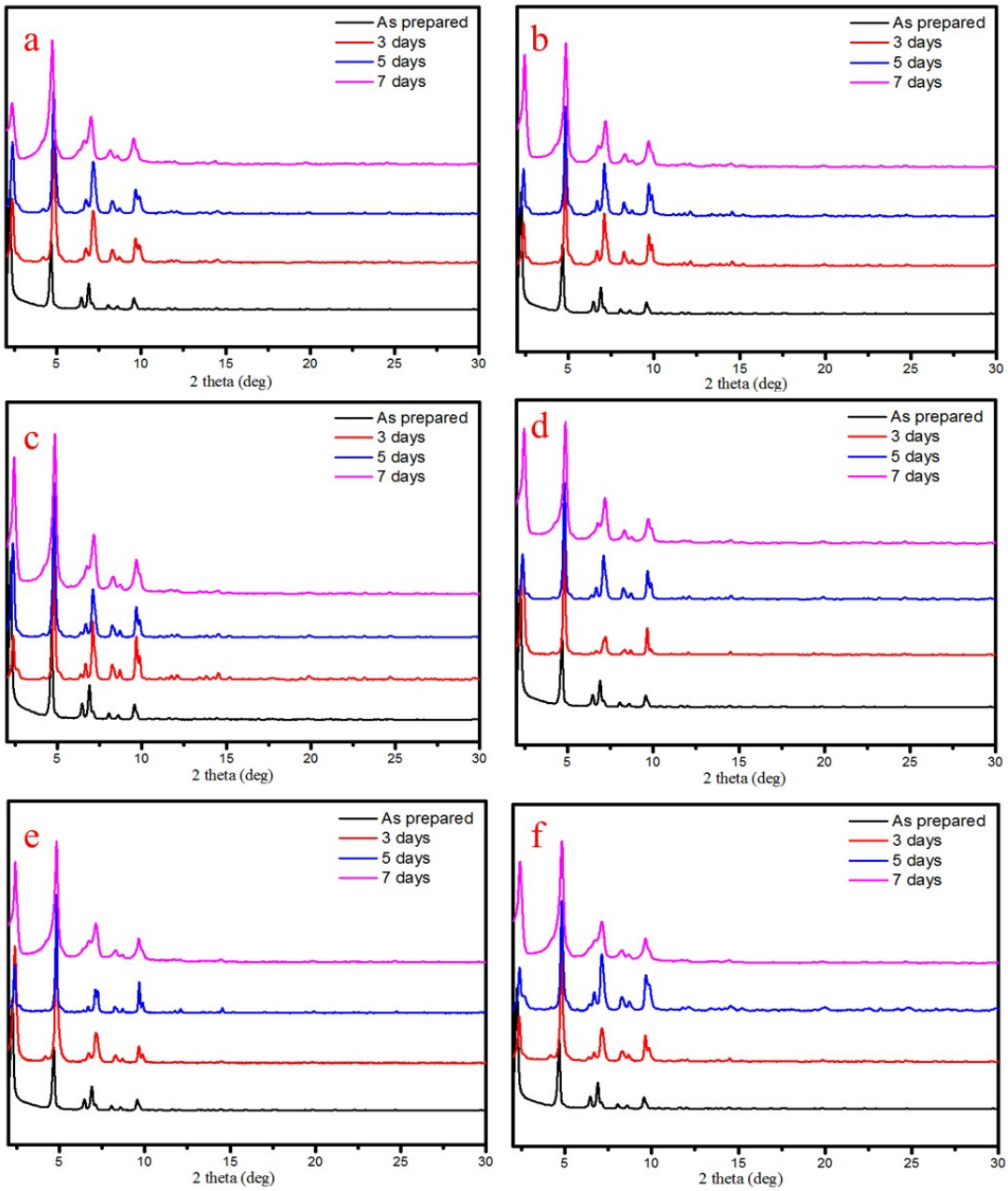

Figure S6. PXRD patterns of Pd-PCN-222(Hf) upon treatment in different solvents: acetone (a), acetonitrile (b), dichloromethane (c), ethyl acetate (d), methanol (e), and water (f).

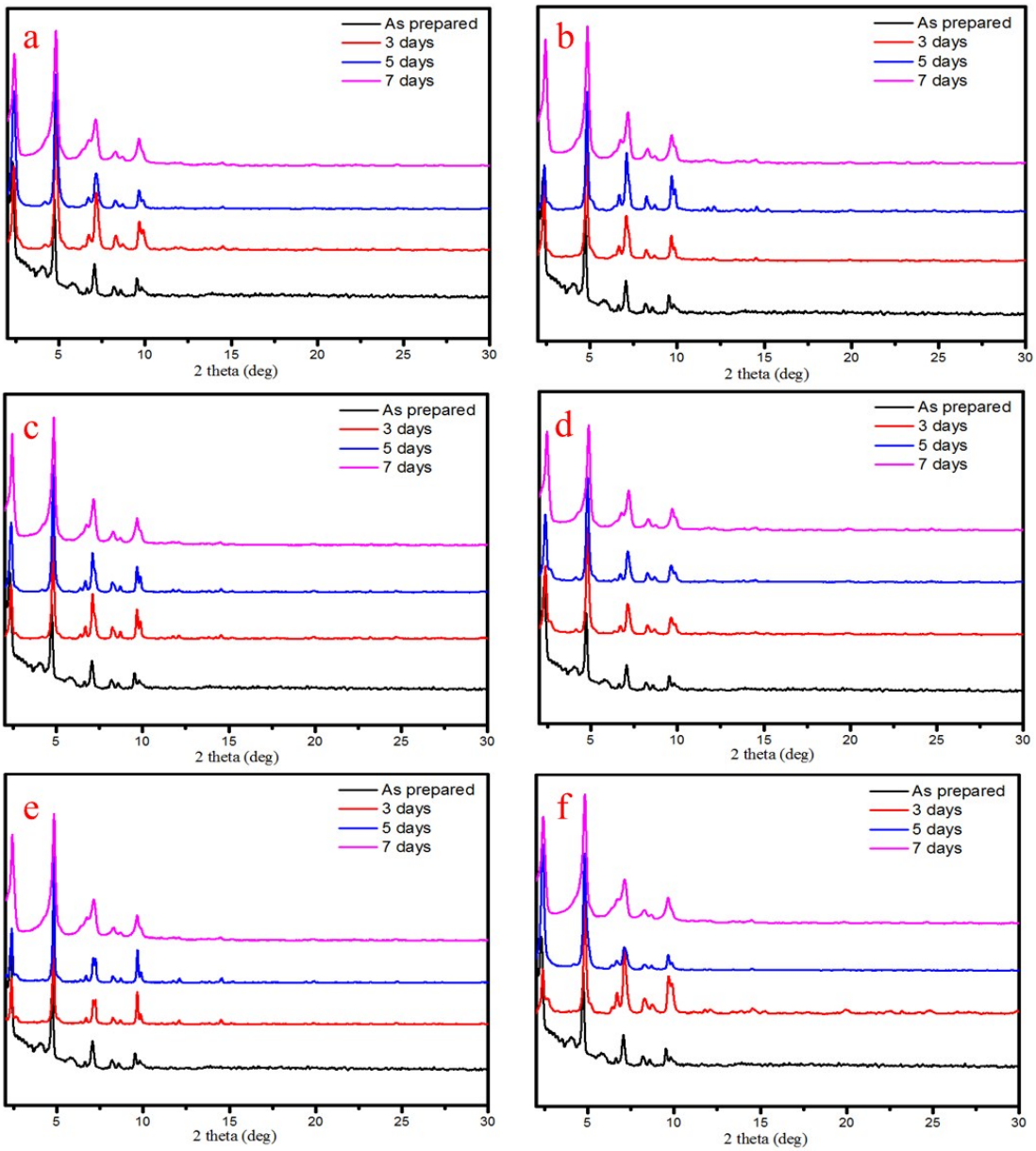

Figure S7. PXRD patterns of Pt@Pd-PCN-222(Hf) upon treatment in different solvents: acetone (a), acetonitrile (b), dichloromethane (c), ethyl acetate (d), methanol (e), and water (f).

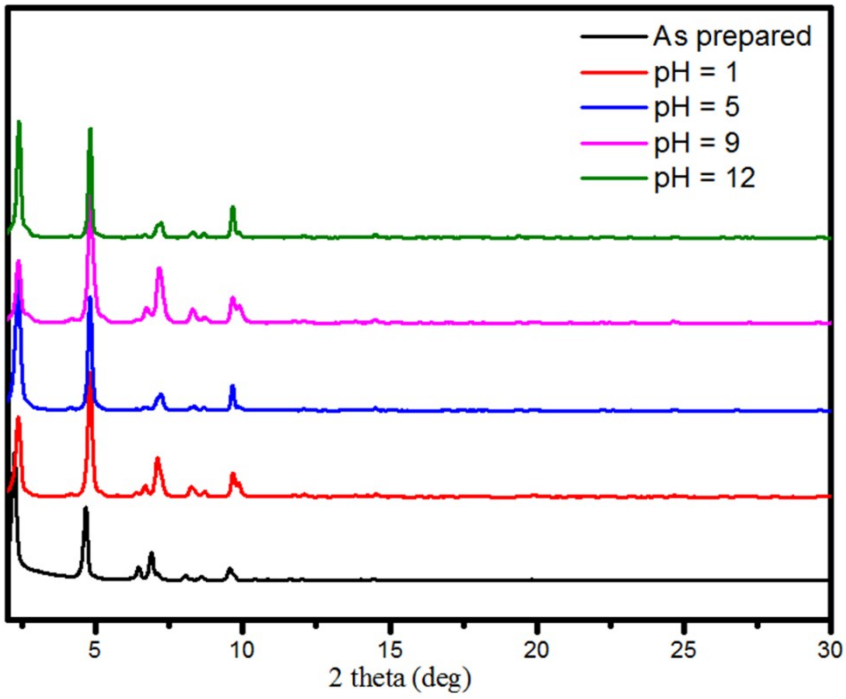

Figure S8. PXRD patterns of Pd-PCN-222(Hf) in aqueous solutions with a pH range of 1-12.

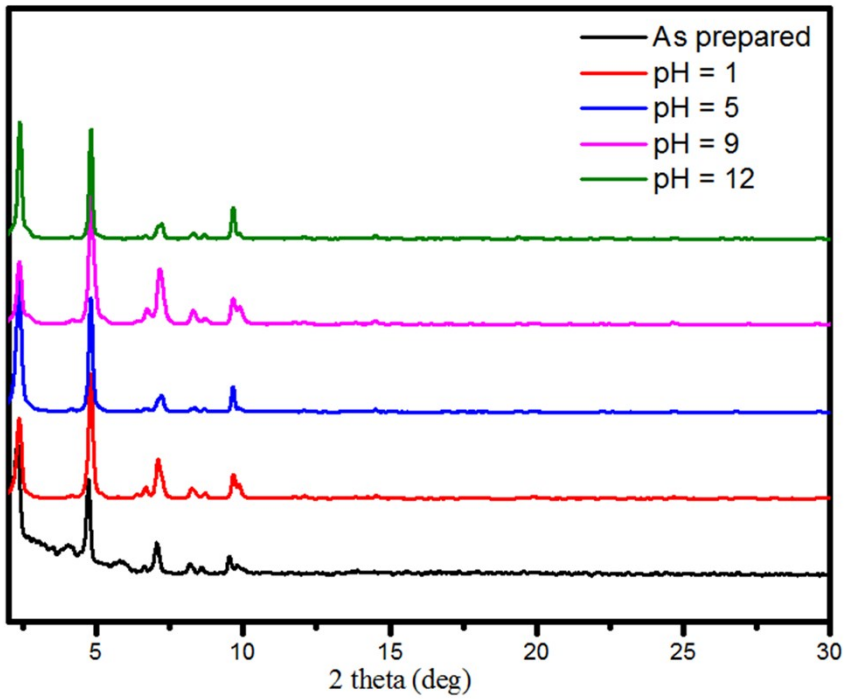

Figure S9. PXRD patterns of Pt@Pd-PCN-222(Hf) in aqueous solutions with a pH range of 1-12.

5. Photocatalytic Reactions

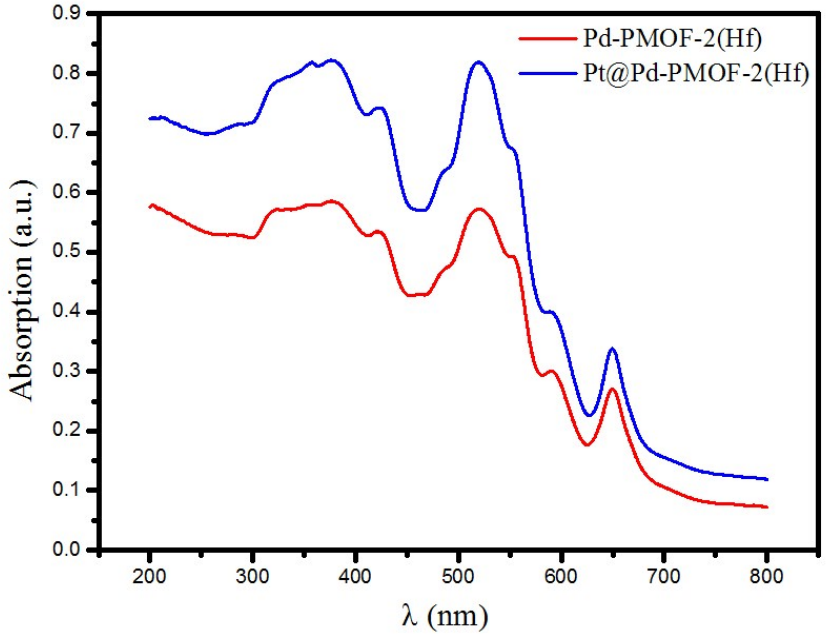

Figure S10. Steady-state UV−vis spectra of Pd-PCN-222(Hf) and Pt@Pd-PCN-222(Hf).

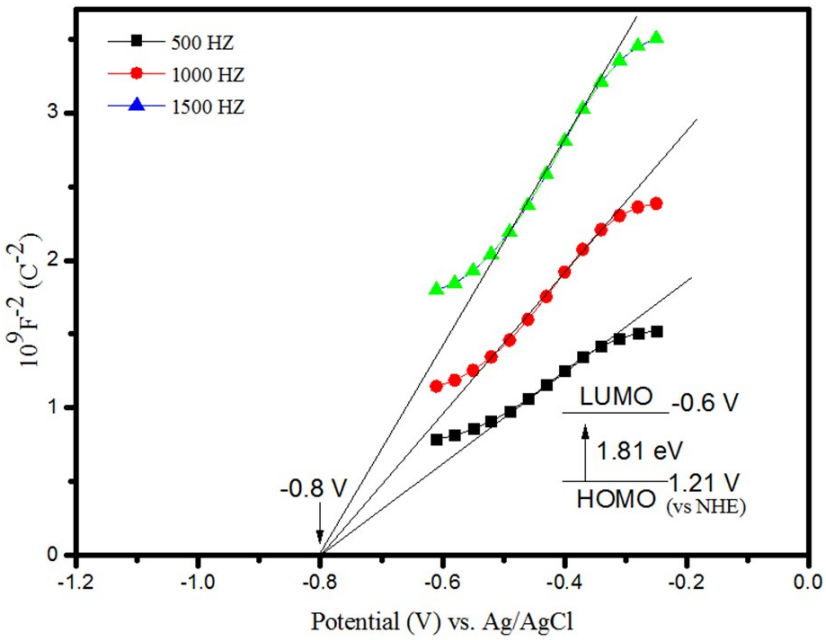

Figure S11. Mott-Schottky plots of PdTMCPP in 0.2 M Na_2SO_4 aqueous solution.

Inset is energy diagram of the HOMO and LUMO levels of PdTMCPP.

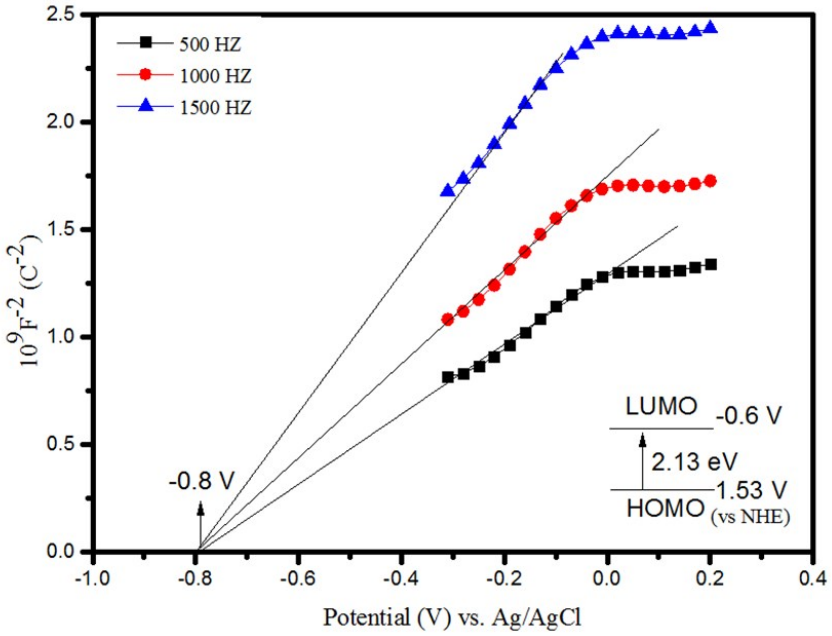

Figure S12. Mott-Schottky plots of Pd-PCN-222(Hf) in 0.2 M Na_2SO_4 aqueous solution.

Inset is energy diagram of the HOMO and LUMO levels of Pd-PCN-222(Hf).

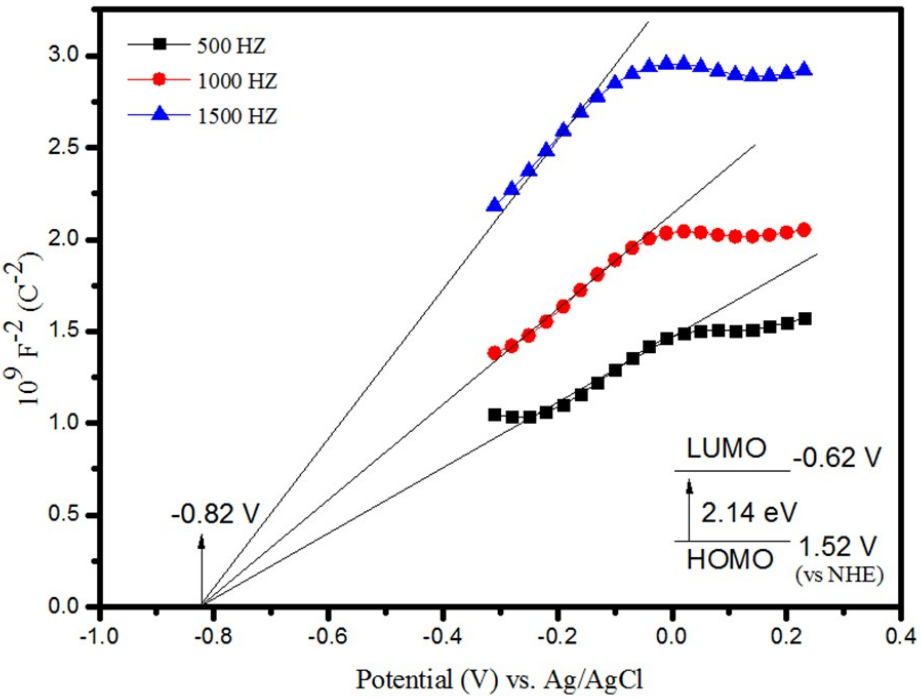

Figure S13. Mott-Schottky plots for Pt@Pd-PCN-222(Hf) in 0.2 M Na_2SO_4 aqueous solution. Inset is energy diagram of the HOMO and LUMO levels of Pt@Pd-PCN-222(Hf).

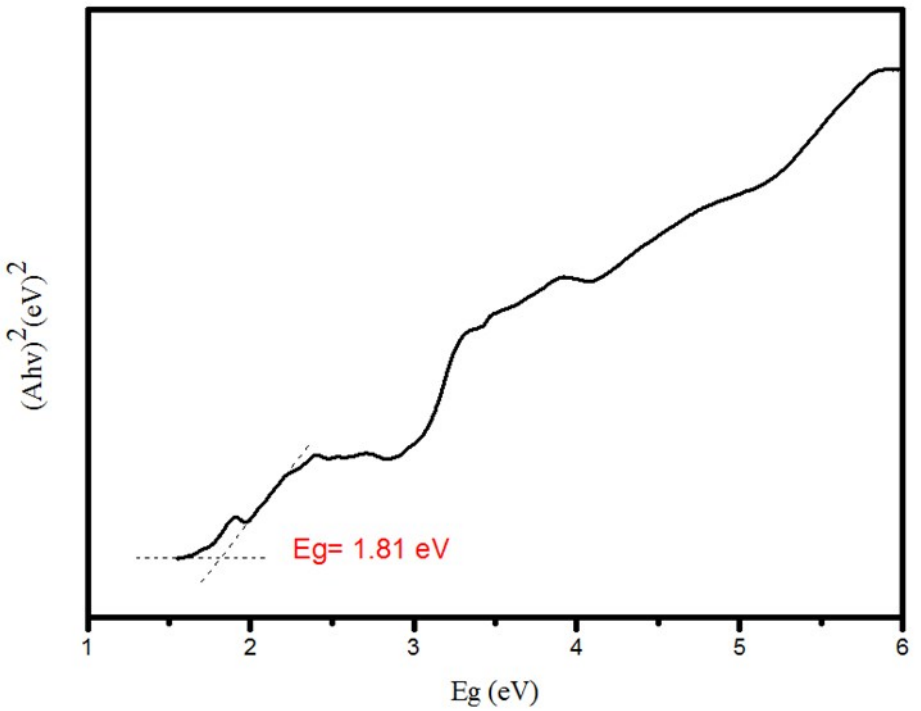

Figure S14. Tauc plot of PdTMCPP.

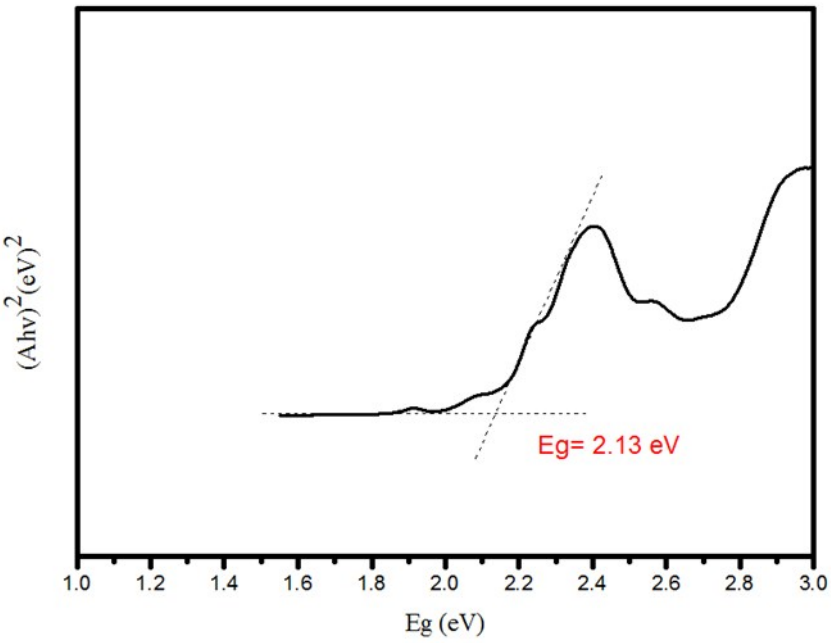

Figure S15. Tauc plot of Pd-PCN-222(Hf).

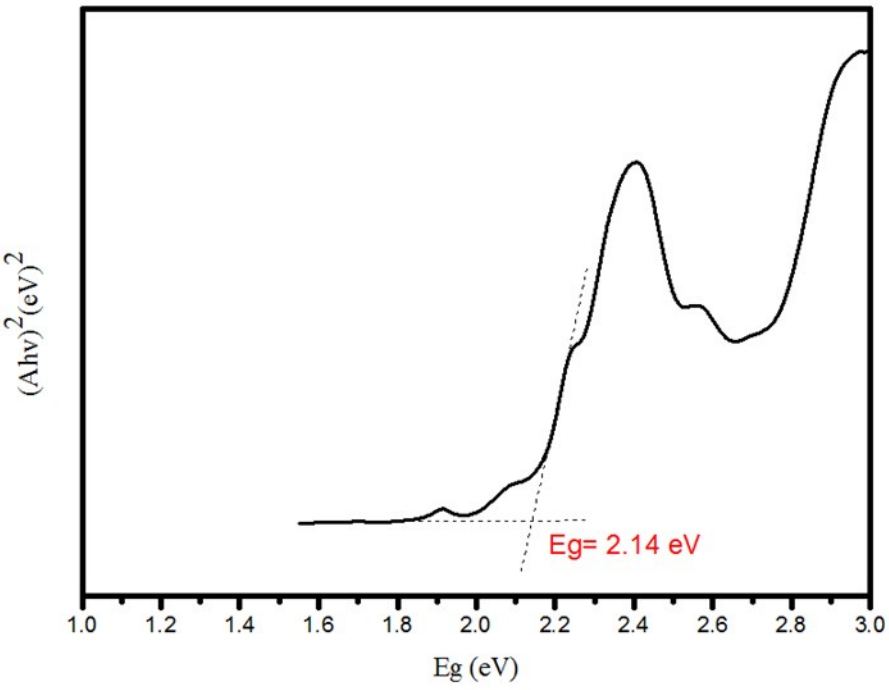

Figure S16. Tauc plot of Pt@Pd-PCN-222(Hf).

Table S2. Optimization of reaction conditions.[a]

Entry	Solvent	$V_{solvent}$ (mL)	V_{H_2O} (μL)	Sacrificial Agent	Sacrificial Agent Amount (mL)	H_2 production rate ($\mu mol \cdot g^{-1} \cdot h^{-1}$)
1	Acetonitrile	10	250	Triethanolamine	2.5	22674
2	Isopropanol	10	250	Triethanolamine	2.5	12600
3	DMF	10	250	Triethanolamine	2.5	12130
4	Acetone	10	250	Triethanolamine	2.5	10073
5	DMAC	10	250	Triethanolamine	2.5	9613
6	DMSO	10	250	Triethanolamine	2.5	2470
7	Pyrrole	10	250	Triethanolamine	2.5	116
8	Acetonitrile	10	250	Methanol	2.5	3220
9	Acetonitrile	10	250	DMA	2.5	90
10	Acetonitrile	10	250	Ascorbic acid	10 mg	< 5
11	Acetonitrile	10	250	BIH	112 mg	11586
12	Acetonitrile	10	225	Triethanolamine	2.5	10436
14	Acetonitrile	10	275	Triethanolamine	2.5	13356
15	Acetonitrile	10	250	Triethanolamine	1.5	15480
17	Acetonitrile	10	250	Triethanolamine	3.5	11000

[a]The reaction is using Pt@Pd-PCN-222(Hf) (5 mg) as the catalyst and under visible light irradiation (≥420 nm) for 3 h.

Table S3. The amount of H_2 produced in different reaction time.

Time (h)	The amount of H_2 produced ($\mu mol \cdot g^{-1}$)	H_2 evolution rate ($\mu mol \cdot g^{-1} \cdot h^{-1}$)
1	18920	18920
2	44017	22008
3	68023	22674
4	77042	19260
5	89985	17997
6	100558	16760
7	106208	15173
8	116077	14510
20	164575	8229
22	174884	7949
24	176140	7339
26	180091	6927
28	186850	6673
30	193833	6461
32	194168	6068

Table S4. H_2 evolution rates of porphyrin-based MOFs.

Entry	Catalyst	H_2 production rate ($\mu mol \cdot g^{-1} \cdot h^{-1}$)
1	PCN-222(Hf)	0
2	Pt@PCN-222(Hf)	441
3	Pd-PCN-222(Hf)	2476
4	Pt@Pd-PCN-222(Hf)	22674

[a]The reaction is using 5 mg catalyst and carried out in the mixed solvent of acetonitrile/water (10 mL/250 μL) in the presence of triethanolamine (2.5 mL) as the sacrificial agent under visible light irradiation (≥ 420 nm) for 3 h

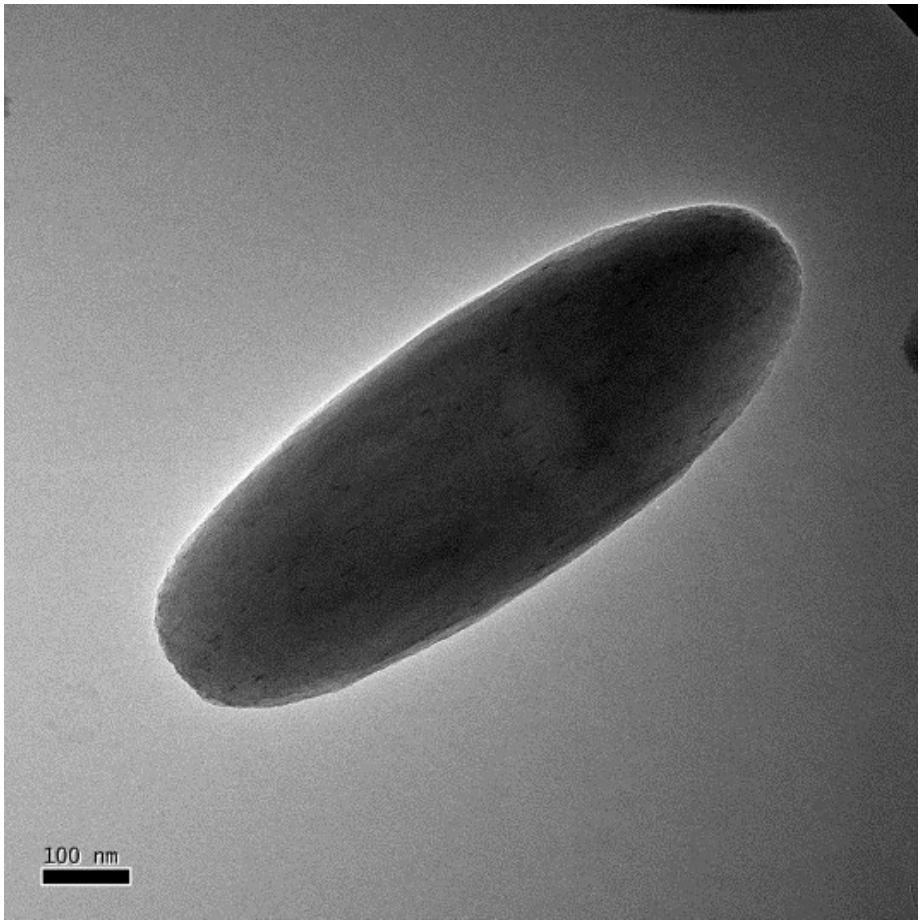

Figure S17. The TEM image of Pt@Pd-PCN-222(Hf) after the first run (3 h).

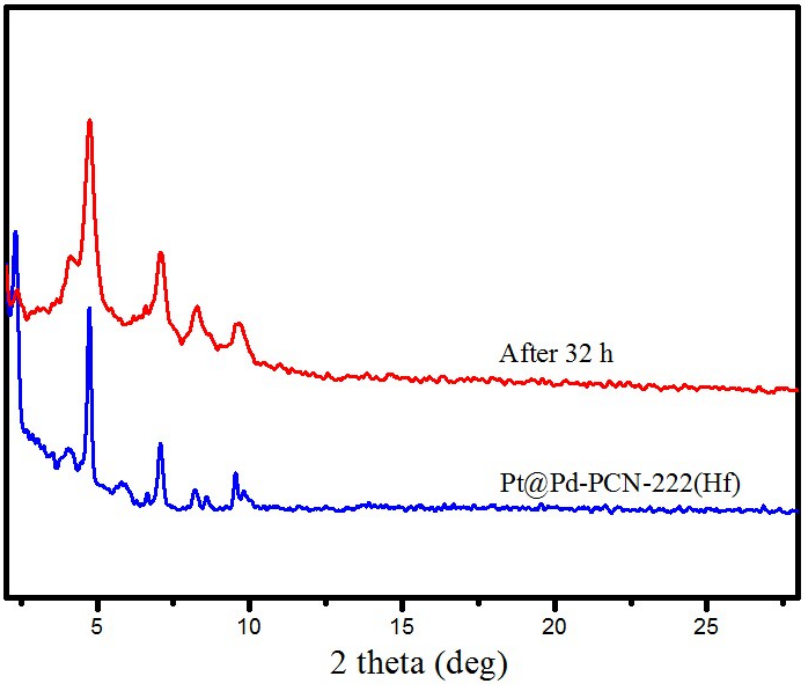

Figure S18. PXRD patterns of Pt@Pd-PCN-222(Hf) after photocatalytic reaction of 32 h.

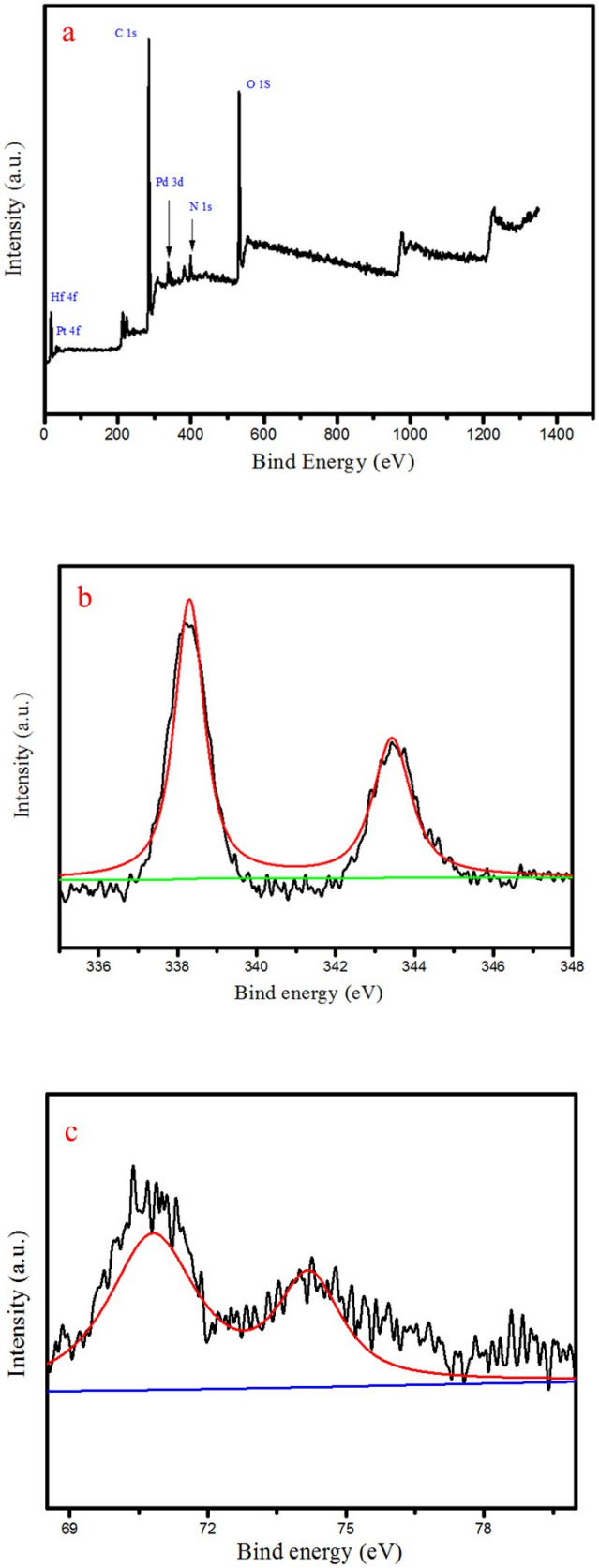

Figure S19. XPS spectrum of Pt@Pd-PCN-222(Hf) after photocatalytic reaction of 32 h.

6. Mechanism Study

Table S5. The TA lifetime of Pd-PCN-222(Hf) and Pt@Pd-PCN-222(Hf).

Sample	τ1 (ps)	τ2 (ps)
Pd-PCN-222(Hf)	17500 (76.7%)	11.4 (23.3%)
Pt@Pd-PCN-222(Hf)	2.19 (16.6%)	7260 (83.4%)

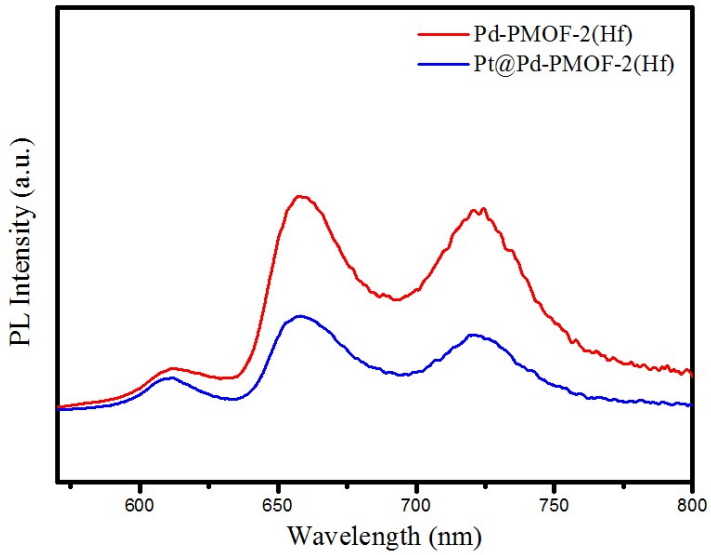

Figure S20. Photoluminescence emission spectra of Pd-PCN-222(Hf) and Pt@Pd-PCN-222(Hf).

Table S6. The PL lifetime of Pd-PCN-222(Hf) and Pt@Pd-PCN-222(Hf) (in the vacuum).

Sample	τ1 (μs)	τ2 (μs)	τ3 (μs)	τ (μs)
Pd-PCN-222(Hf)	0.8681(24.48%)	10.7177(14.69%)	183.548(60.83%)	113.4
Pt@Pd-PCN-222(Hf)	0.8448(45.23%)	10.8696(20.15%)	257.235(34.62%)	91.6

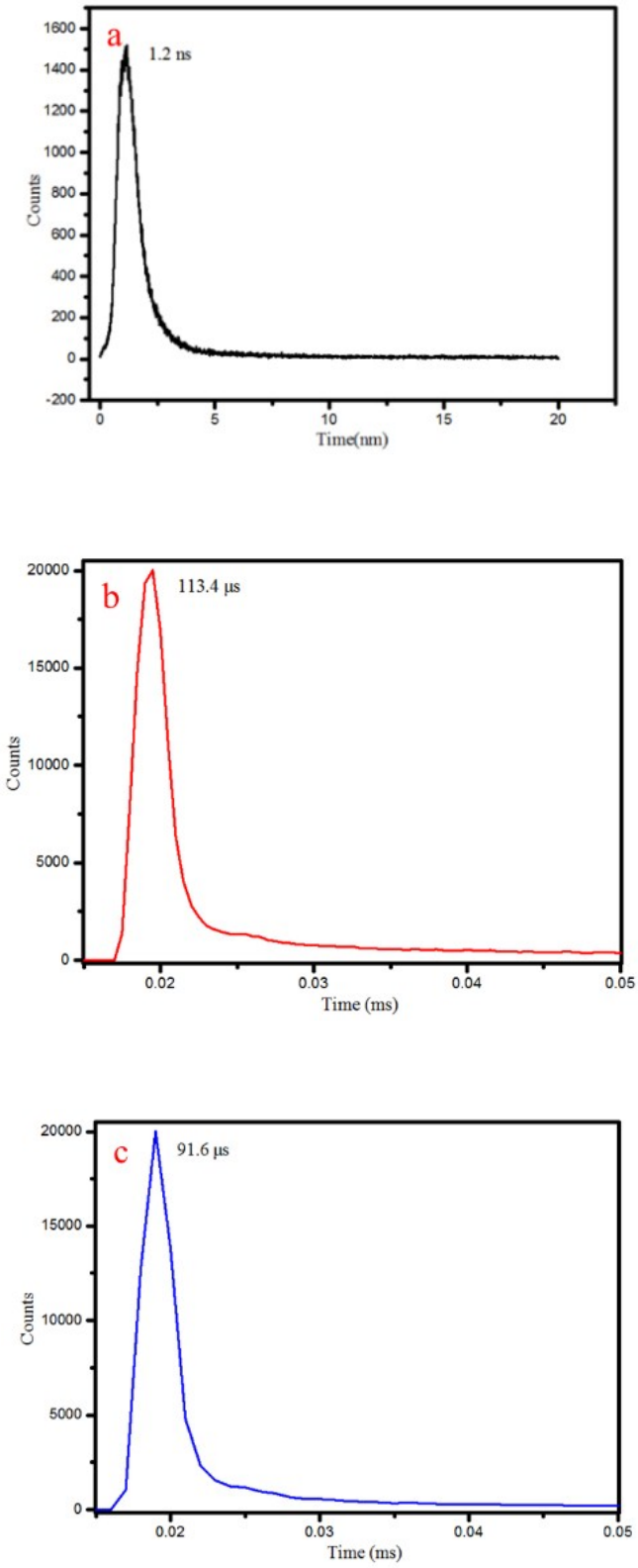

Figure S21. Emission decay of PCN-222(Hf) (a), Pd-PCN-222(Hf) (b) and Pt@Pd-PCN-222(Hf) (c) at 298 K under vacuum.